redin Revista Facultad de Ingeniería, Universidad de Antioquia, No.89, pp. 9-15, Oct-Dec 2018

Study of the influence of cobalt in the high formability of the Au-Fe system

Estudio de la influencia de cobalto en la alta deformabilidad del sistema Au-Fe

Sandra Milena Restrepo-Arcila[1,3*], Alejandro Iván Echavarría-Velásquez[2], Héctor Darío-Sánchez Londoño[2], Marco Antonio Giraldo-Cadavid[1]

[1]Facultad de Ciencias Exactas y Naturales, Universidad de Antioquia. Calle 67 # 53-108. A. A. 1226. Medellín, Colombia
[2]Facultad de Ingeniería, Universidad de Antioquia. Calle 67 # 53-108. A. A. 1226. Medellín, Colombia
[3]Facultad de Minas, Universidad Nacional de Colombia, Sede Medellín, calle 80 # 65-223. A.A. 1027. Medellín, Colombia

ARTICLE INFO:
Received: October 19, 2017
Accepted: August 14, 2018

AVAILABLE ONLINE:
November 09, 2018

KEYWORDS:
Metallurgy, gold alloys, as-cast, heat-treatment, jewelry

Metalurgia, aleaciones de oro, as-cast, tratamiento térmico, joyería

ABSTRACT: Since ancient times, gold has been used due to its especial properties. Among those properties are the resistance to corrosion (for being noble), its high electrical and thermal conductivity, and also its conspicuous coloration. Gold has been applied in a diversity of subjects such as economy, jewelry, electronic circuits and odontology. The fascinating properties of gold are likely to improve with the preparation of alloys; among those, the Au-Fe alloys constitute some of the most studied nowadays. In this research, we present our results concerning the microstructure of the Au-Fe and Au-Fe-Co alloys. We fabricated gold based alloys with 25% (weight) Fe and then compared their structure and formability to Au-24.5Fe-0.5Co (% weight) to determine the role of cobalt in the alloy. An induction furnace with controlled atmosphere (argon) and conductor crucibles coated with zirconium silicate was used. The samples were characterized by three processes: *as-cast*, with heat treatment (HT) at T=900°C (1h and 3h) and *as-cast centrifuged*.

The formability results for the *as-cast* samples revealed a 23% deformation (rolling mill) for the Au-25Fe versus a 62% for the Au-24.5Fe-0.5Co alloy (HT-1h; T=900°C), whilst for the *as-cast centrifuged* sample revealed a 75% deformation with ductile fracture for the Au-25Fe versus an 82% without fracture for the Au-24.5Fe-0.5Co alloy. This result is particularly promissory for the applications in jewelry, showing that the addition of cobalt increases the formability of Au-Fe alloys.

RESUMEN: Históricamente el oro ha sido usado debido a las especiales propiedades que posee, entre las que se pueden resaltar su resistencia a medios agresivos (por ser altamente inerte), su buena conducción térmica y eléctrica, y porque además presenta un color llamativo. Sus principales aplicaciones se han dado en áreas como la economía (en el uso de monedas), en joyería, en electrónica y en odontología. Con el fin de mejorar las propiedades que presenta el oro, se fabrican aleaciones de éste con otros metales. Dentro de las nuevas aleaciones que se están desarrollando, se encuentra el sistema de aleaciones Au-Fe. En esta investigación se pretende profundizar en el estudio de la microestructura de las aleaciones Au-Fe y Au-Fe-Co, para lo cual, se fabricaron aleaciones base oro aleadas con 25% (p/p) Fe y se han comparado a nivel de estructura y conformabilidad con la aleación Au-24.5Fe-0.5Co (% p/p), con el fin de determinar la influencia de este último aleante (el cobalto). Las aleaciones se obtuvieron en horno de inducción con atmósfera controlada de argón, utilizando crisoles conductores revestidos con silicato de zirconio. Las muestras se caracterizaron en tres diferentes procesos: *as-cast* con tratamiento térmico a temperaturas de 900°C a una y tres horas respectivamente y *as-cast* centrifugada. Los resultados de conformabilidad al finalizar el proceso son 62% de deformación (en laminador) para la aleación Au-24.5Fe-0.5Co contra el 23% para el sistema Au-25Fe para las muestras obtenidas *as-cast* y con tratamiento térmico a 900°C por 1 hora.

* Corresponding author: Sandra Milena Restrepo Arcila
E-mail: sandra.restrepoa@udea.edu.co
ISSN 0120-6230
e-ISSN 2422-2844

DOI: 10.17533/udea.redin.n89a02

Las muestras *as-cast* centrifugadas presentaron una deformación de 75% con fractura dúctil en Au-25Fe y de 82% sin fractura en Au-24.5Fe-0.5Co. El anterior resultado es satisfactorio para el sistema con adición de cobalto, lo cual es altamente benéfico para diversas aplicaciones, sobretodo la joyería.

1. Introduction

Although gold has been known and used by humankind since ancient times, new special properties of gold alloys have arisen during the last decade, mainly due to their fine structure. Among those new gold-based alloys, the Au-Fe system receives special attention thanks to its magnetic behavior and nano-structured organization [1].

In this study, we focused on the Au-Fe system and Au-Fe alloys with addition of cobalt (5% on the Au-25Fe system), which are of interest in a diversity of disciplines, due to their wide range of applications.

1.1 The Au-Fe system

In the Au-Fe alloys, the microstructures in *as-cast* condition exhibit ferrite α (BCC) and solid solution of Au(Fe) (FCC). The existence of (α)ferrite increases directly with the content of iron. Figure 2 shows the role of the α phase BCC in the structure of the Au-Fe alloys, determined with XRD and the theoretical predictions of the phase diagram depicted in Figure 1 [2]-[3].

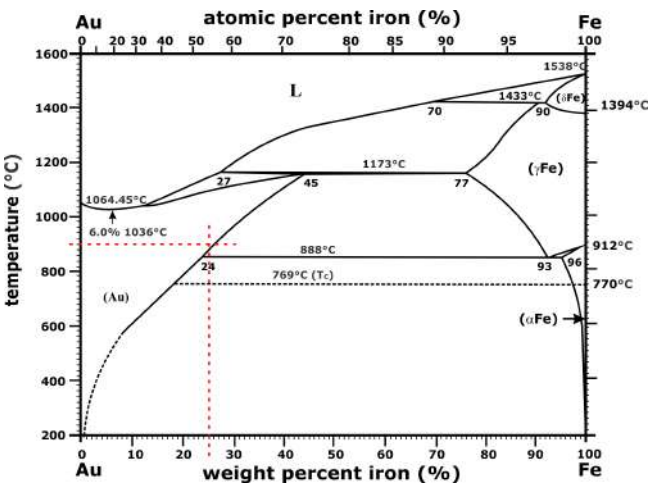

Figure 1 Phase diagram Au-Fe. The treated system alloy in this study falls into the Au-solid solution. The orange horizontal line at 900°C intercepts the vertical one that refers to composition (75% Au, 25% Fe). Figure was traced from [2]

Au-11Fe (% weight)

For this alloy, initially obtained with the Melt Spinning technique (TT; T=320°C, 168h), ferrite BCC acicular are precipitated. The acicular are about 5-10 nm thick and ca. 50 nm long, embedded in an Au FCC matrix (Figure 2) [3].

As observed from Figure 2, the proportional amount of ferrite is of about 10%, which agrees with the value expected from Figure 3[4].

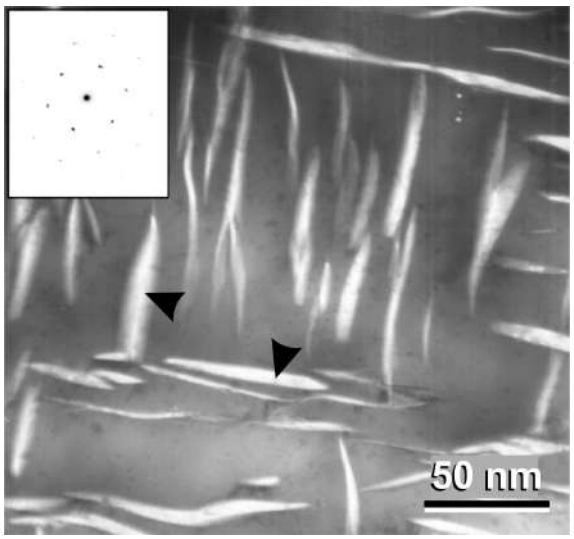

Figure 2 TEM micrograph for the Au-11Fe alloy (% weight) with heat treatment at 320°C during 168 h. The acicular structural morphology of the ferrite is observed (white areas arrowheads). Inset: Scheme of the FCC structure characteristic of gold. Image taken and reorganized from [3]

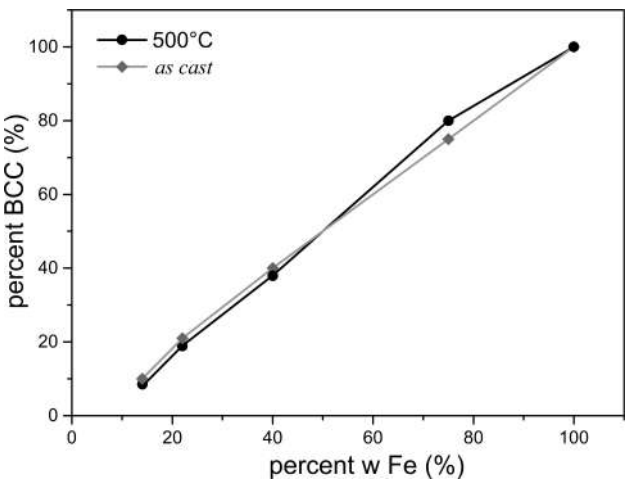

Figure 3 Participation of the α phase BCC in the Au-Fe alloys structure determined with XRD (squares, gray) and theoretical prediction of the phase diagram shown in Figure 1 (circles, black). Image plotted from table in [4]

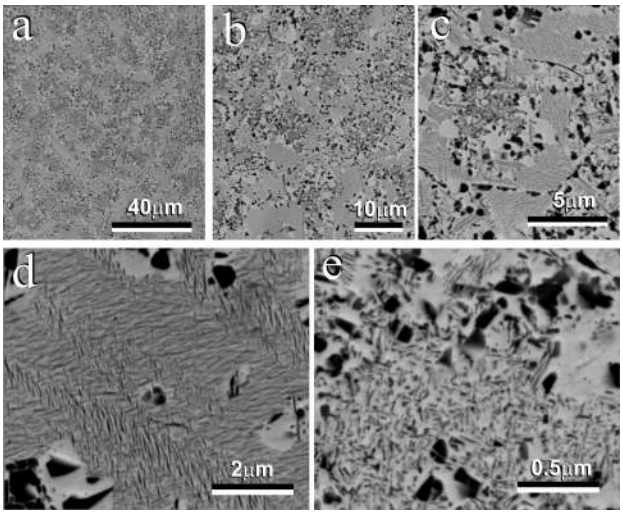

Figure 4 SEM micrographs of the Au-22Fe (% weight) alloy heat treated at 500 °C during 48 h. Images taken and reorganized from [4]

Au-22Fe (% weight)

In close agreement with Figure 1, in this alloy the first dendrites are formed with iron content close to 30%, whilst the proportion is about 15% for the interdendritic areas, the last to be formed. The microsegregation inside the dendrite is evident from Figure 4 (a, b, c and d) [4]. The dendrites, iron-rich, appear darker in the SEM micrograph (Figure 4 b, c) and the interdendritic composite, of lighter appearance, has less iron content.

The darker areas, iron-rich, precipitate the eutectoid composite (Figure 4c, d); more clearly observed in Figure 4f, according to the Equation. (1)

$$Fe\,(\gamma) \rightarrow Fe\,(\alpha) + (Au) \quad (1)$$

In Figures 4c and 4d, the lighter old-rich regions correspond to the interdendritic composite, which precipitate Fe(α) from the solid solution (Au), according to the Equation. (2)

$$(Au) \rightarrow Fe\,(\alpha) + Au \quad (2)$$

The precipitation of Fe(α) from the solid solution Au (FCC) shows the same laminar morphology than that shown in Figure 3 for the 11% Fe system, although here the presence of Fe(α) is higher, of about 35%.

Au-40Fe (% weight)

The SEM micrographs corresponding to an alloy Au-40Fe (% weight) in *as-cast* (Figure 5), show the dendrites of the austenite primary γ-FCC (dark) and the interdendritic composite (light) Au(Fe) FCC (Equation. (3)). The peritectic reaction is evident in the light area around the dendrite (dark areas in Figure 5a, b and magnified in Figure 5c) [5].

$$Fe\,(\gamma) + L \rightarrow Fe\,(\gamma)\ at\ 1173^{\circ}C\ and\ 40\%Fe \quad (3)$$

Subsequent cooling causes gold precipitation according to the Equation (4)

$$Fe\,(\gamma_{initial}) \rightarrow Fe\,(\gamma_{final}) + (Au) \quad (4)$$

Finally, the eutectoid reaction occurs starting from $Fe(\gamma_{final})$ and the precipitation of acicular ferrite from the solid solution (Au). All the reactions according to the phase diagram of the Au-Fe system of Figure 2.

Figure 5 shows the eutectoid Au in detail. The precipitation of the acicular ferrite from (Au), is observed in Figure 5d [4, 5].

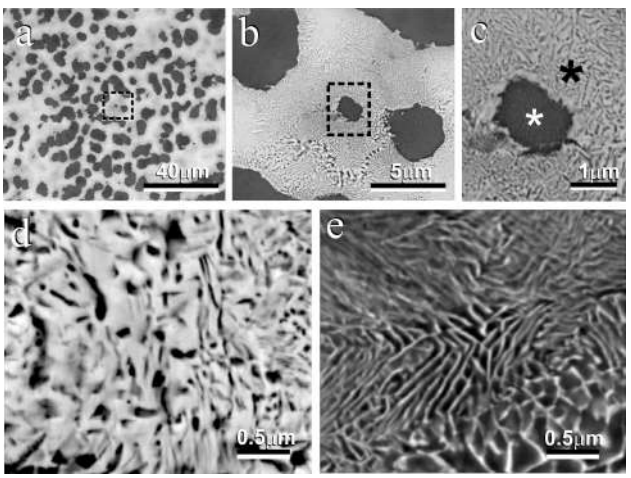

Figure 5 SEM micrographs of the alloy Au-40 Fe (%w) *as-cast*. (a-c) Magnifying sequence of a dendrite. (d) Magnified interdendritic area corresponding to the black asterisk in (c). (e) Magnified dendritic area corresponding to the white asterisk in (c). Dendrites from the primary austenite γ-FCC, which appear dark and surrounded by the white phase Au(Fe) FCC (a-c), are transformed into laminar eutectoide during cooling (e). Figure (b) and (c) correspond to the dashed squares in (a) and (b) respectively. Images taken and reorganized from [4]-[5]

1.2 The influence of cobalt in gold alloys

It is known that when cobalt is added in alloys of the Au-Ag-Cu system (14-18 karats) in concentrations smaller than 0.5%-weight, it acts as a grain refiner. Cobalt also acts as an effective grain refiner during the soft reheating stage (recrystallization) when the material is worked cold between 0.15 and 0.50 %Co [6].

It has been reported that cobalt improves formability in gold alloys for concentrations lower than 1.5% [7–9]. However, the possible role of cobalt in Au-Fe-Co alloys

as grain refiner and improver of formability has not been explored so far. The main objective in this research was to evaluate the influence of an addition of 0.5% Co % weight to an Au-24.5% Fe alloy on formability and strength.

2. Materials and methods

Au-24.5Fe-0.5Co y Au-25Fe (% weight) alloys were obtained for fusion by induction in argon atmosphere. Refined gold was obtained by quartering and subsequent dissolution in nitric acid [9]. As additives we used iron 99.95% (Baker Chemical Co) and micronized cobalt 99.9% (Goodfellow Cambridge Ltd). Graphite crucibles coated with bonded zirconia-colloidal silica (Ludox SM, Du Pont) were used to avoid iron or cobalt contamination. The melted components were then centrifuged in the furnace and deposited in a cylindrical metal mold of 5mm diameter and approximately 15 mm long. The *as-cast* samples were cooled down slowly inside the furnace keeping a constant flow of argon to avoid oxidation. After fusion and structural characterization, the samples were heat treated at 900°C for 1 and 3 h.

In order to obtain the *as-cast centrifuged samples*, and subsequently tempered, a copper mold cylinder-shaped was used. The sample obtained was divided in smaller cylindrical pieces 3mm long (six pieces), and each was deformed in a roller mill (three pieces) and by hydraulic compression (the other three) at 140 ksi.

For the structural characterization under scanning electron microscopy, the samples were gently polished until obtaining a mirror finishing and then attacked with *aqua regia* to reveal the structure.

To represent the ternary diagram of the Au-24.5Fe-0.5Co system, the *FactSage* thermochemical software and databases were used, under the following conditions: 1200°C (fusion) and 900°C (heat treatment) at 1 atmosphere of pressure.

3. Results

The Au25Fe system must have a similar morphology to that of the Au22Fe, already widely studied and reported [2, 3]. The first dendrites to be formed are $\gamma - Fe$ (or acicular ferrite) (Figure 5a, dark areas), which are surrounded by the rich gold phase (Figure 5a, whitish areas), as concluded from the AuFe system phase diagram (Figure 1). For our Au25Fe sample obtained *as-cast* (Figure 6), these two phases are present. The darker area in Figure 6b (interdendritic zone) corresponds to the eutectoid reaction.

It is evident from Figure 7, the beneficial effect of adding cobalt to the system (0,5% in this case), since a refined morphology is clearly observed in the SEM micrographs. Although the magnifying sequence of images in Figure 6 (*as-cast*, without Co) displays a dendritic phase, that is not the case in the sequence in Figure 7 (*as-cast*, with Co). However, a heat treatment of the sample (Figure 9) reveals thin dendrites by augmenting the relative area occupied by the interdendritic zone.

A change in the way the ferrite precipitates from the solid solution (Au) is appreciated in the sample *as-cast* with cobalt (Figure 7a,b), which favors the eutectoid reaction.

A different morphology for the metastable eutectoid appears in the Au-25Fe sample (Figure 8), which was heat-treated for one hour, and cooled down in water. This morphology appears presumably due to the rapid cooling, for which the metastable eutectoid phase displays a different morphology to that shown in Figure 4, 5 and 6.

In comparison, micrographs for the cobalt-added sample (Au-24.5Fe0.5Co) are shown in Figure 9. Here, the effect of the heat treatment is also evidenced by a larger amount of the metastable eutectoide phase.

A refining of the microstructure in the iron-rich phase is observed in the samples *as-cast centrifuged* with cobalt (Figure 10 a, b).

In order to compare the hardness of the samples *as-cast*-HT-3h and *as-cast centrifuged*, they were subjected to the Vicker´s hardness test, as measured with the micro-hardness tester (Tables 1 and 2, and Figure 11).

For the *as-cast* samples, the one with the addition of cobalt is also the harder. Subsequent heat treatment hardens the samples, presumably due to the significant augment of the Au(Fe) phase.

Table 1 Hardness results for the Au-25Fe (% weight) alloy. The Vicker´s micro-hardness test was applied

	Hardness (HV)			
	as-cast	**HT 1h**	**HT 3h**	**Centrifuged and Tempered**
Au-Fe	85.2	180	206	79
	83	181	207	80
	80.2	181	208	80
Average	82.8	180.7	207	79.7
Standard deviation	2.51	0.58	1	0.58

Figure 12 shows optical microscopy photographs of the Au-25Fe after being deformed for samples without and with cobalt (Figure 12a and 12b, respectively). No fracture is observed in the sample with cobalt (Figure 12b), which

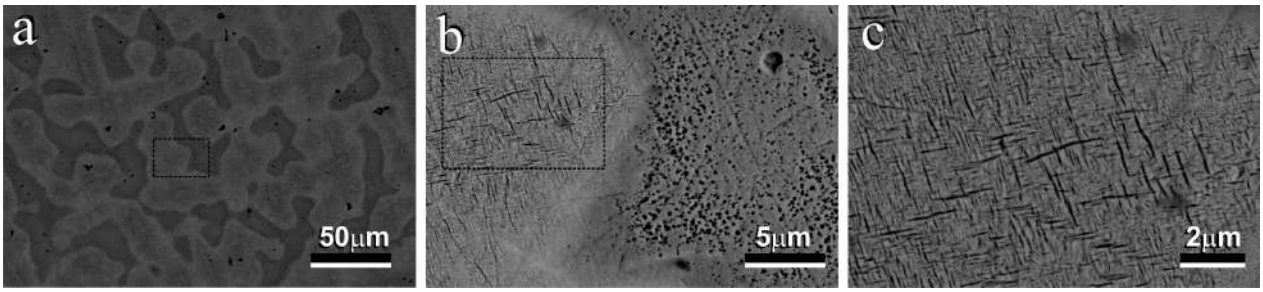

Figure 6 Magnifying sequence SEM Micrographs of the Au-25Fe (% w) *as-cast* sample. (a) Dendritic structure, (b) acicular ferrite (light) and eutectoid composite (dark), corresponding to the dashed square in (a). (c) Augmented acicular ferrite zone, corresponding to the dashed square in (b)

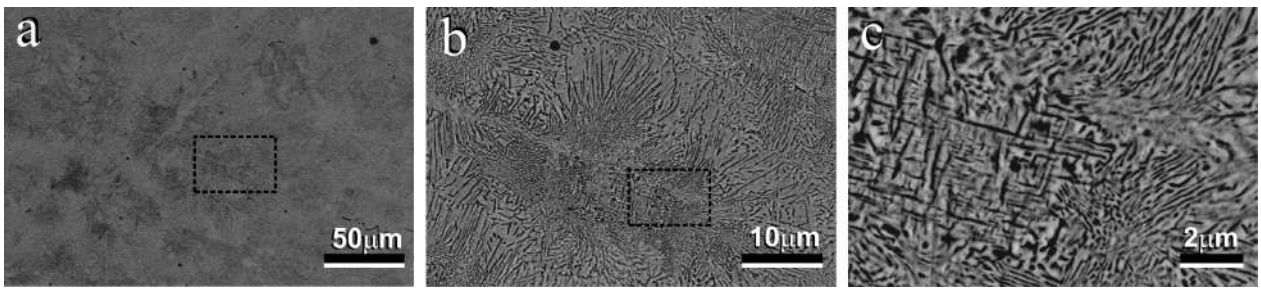

Figure 7 Magnifying sequence SEM Micrographs of the Au-24.5Fe-0.5Co (%w) *as-cast* sample. A refining effect is observed compared to the one without cobalt in Figure 6. Figures (b) and (c) correspond to dashed squares in (a) and (b), respectively

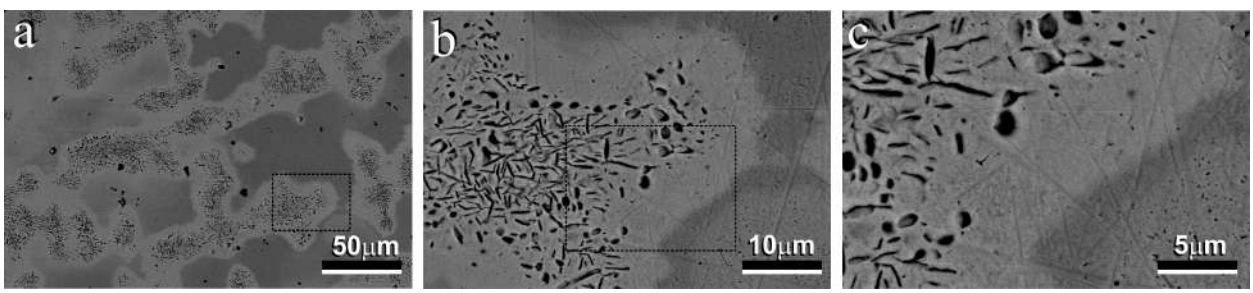

Figure 8 Magnifying sequence SEM micrographs of the Au-25Fe (%w) sample, HT-1h. The heat treatment produces a globulization of the acicular ferrite, which is more evident in the border zone of the dendrite. Figures (b) and (c) correspond to dashed squares in (a) and (b), respectively

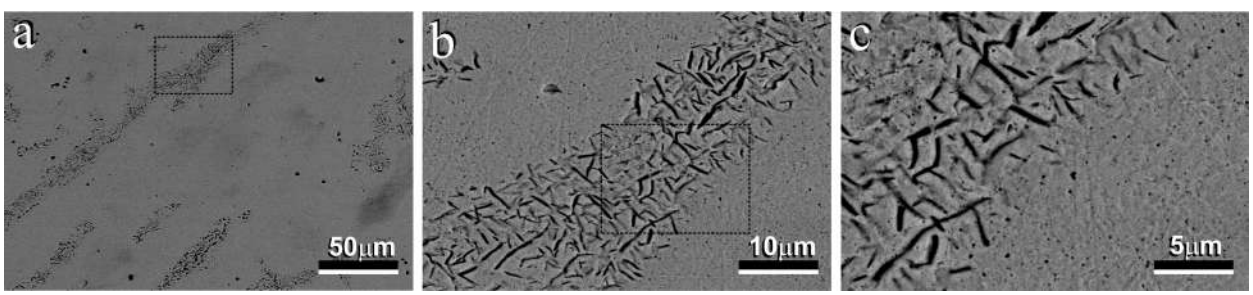

Figure 9 Magnifying sequence SEM micrographs of the Au-24.5Fe-0.5Co (%w) sample, HT-1h. The heat treatment dissolves the α-Fe in the gold matrix. Figures (b) and (c) correspond to dashed squares in (a) and (b), respectively

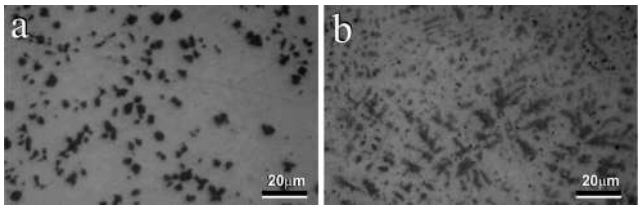

Figure 10 SEM micrographs of the Au-25Fe (%w) and Au-24.5Fe-0.5Co (%w) *as-cast centrifuged* with (b) and without (a) cobalt. The refining effect of centrifuging is evident in both samples compared to the as-cast samples

Table 2 Hardness results for the Au-24.5Fe-0.5Co (% weight) alloy. The Vicker´s micro-hardness test was applied

	Hardness (HV)			
	as-cast	**HT 1h**	**HT 3h**	**Centrifuged and tempered**
Au-Fe-Co	104	170	185	75
	102	170	184	76
	106	170	185	76
Average	104	170	184.7	75.7
Standard deviation	2	0	0.58	0.58

is interpreted as a result of both heat treatment and the cobalt addition itself. On the other hand, the heat treatment alone induces to have a ductile instead of a brittle fracture (Figure 12a).

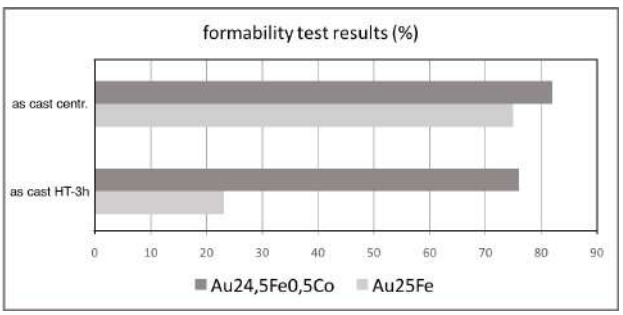

Figure 11 Compared formability of two of the samples (HT-3h: down; centrifuged: up), as deformed with: *as-cast* (rolling mill) and *as-cast centrifuged* (hydraulic press). The showed results correspond to the samples with (dark grey) and without cobalt (light grey)

Figure 13 shows the ternary diagram AuFeCo a (900°C, 1 atm), in which the BCC region (represented by the triangle at the right) receives the ternary point corresponding to our concentrations (Au-24.5Fe-0.5Co). Under these conditions, thus, the crystalline structure is BCC, for which there is no compact planes, leaving the planes with large interplanar separations as the responsible for deformability. This is in fact the reason for the high hardness of the sample.

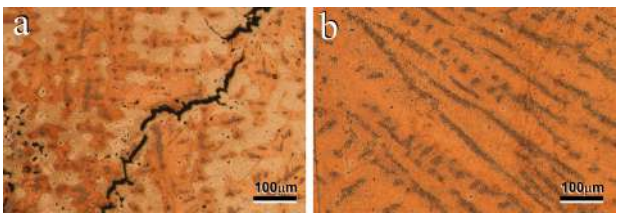

Figure 12 Optical micrographs of the Au-25Fe (a) and Au-24.5Fe-0.5Co (b) samples, HT-3h after deformation by hydraulic compression. Ductile fractures can be seen in (a) but not in (b) which makes evident the effect of the cobalt addition and the heat treatment in the system

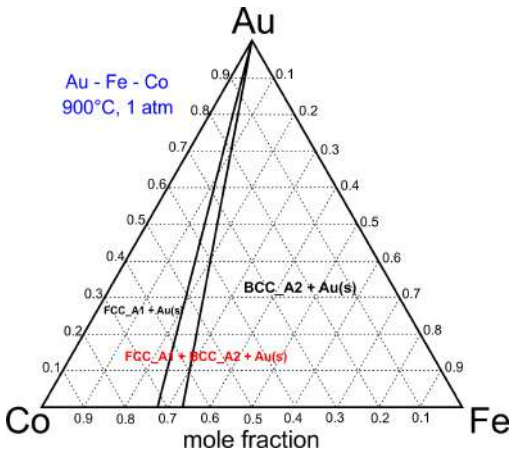

Figure 13 Ternary diagram of the Au-Fe-Co, 900°C and 1 atm

Figure 14 shows the ternary diagram AuFeCo a (1200°C, 1 atm), for the centrifuged Au-24.5Fe-0.5Co. The corresponding structure is then FCC, which is the same structure of pure gold.

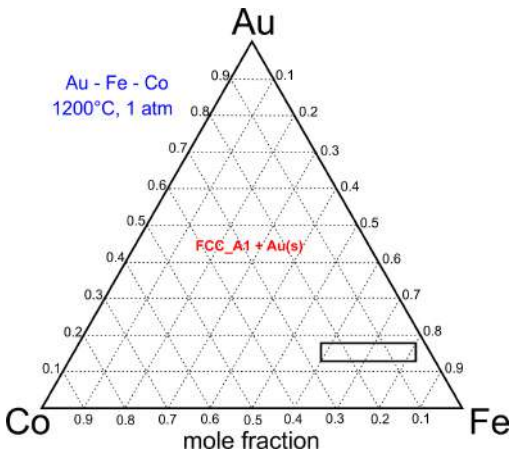

Figure 14 Ternary diagram of the Au-Fe-Co, 1200°C and 1 atm

4. Discussion

Although the function of cobalt as a structure refiner of gold alloys has been studied [7–9], the effects of cobalt in the AuFe system have not been reported before. A question arises: Why is this system important? We propose that the answer lays in the wide range of colors that AuFe alloys generate [10], which is much appreciated in jewelry. Here we have tackled the effects of cobalt on the structure and performance of these alloys.

The presence of laminar eutectoide in the center of the dendrite, for the heat-treated samples, indicates that the first solid to form had the highest concentration of iron (about 42%, Figure 1), indicating the most fragile part of the structure (arrow in Figure 8b).

From the three samples obtained, the one with the best performance was the *as-cast centrifuged* (i.e. rapid solidification); Table 1 and 2, and Figure 11 summarize the results. The heat treatment performed on the *as-cast* sample increases the hardness, but also gives a higher formability since it favors a globulization of the acicular ferrite. However, this new value does not surpass the formability that possesses the *as-cast centrifuged*, which is always higher (Figure 11). A high formability is obtained even for the not-added sample, with a 76% (with fractures, Figure 12a), although the presence of cobalt enhances it to a value of 82% (without fractures, Figure 12b). This fact is highly beneficial for a diversity of applications, from artwork (jewelry) to magnetoresistive materials. However, the heat treated as-cast samples (1h and 3h) resulted in a higher jump of the formability, since a 75% formability was obtained compared with a 23% of the not-added sample.

A better formability can be explained by considering the refining effect of the grain and a smaller presence of a dendritic component in the structure. Also, the change in the crystalline structure of the not-centrifuged sample (BCC) explains the high hardness acquired.

5. Conclusions

We have shown that the addition of cobalt as an alloying in the AuFe system, permits to have a finer structure in the condition as-cast, while keeping the dendritic morphology. By comparing Figures 8 and 9, it is clear that the cobalt makes dendrites thinner, changing the morphology of the alloy.

Regarding the interdendritic area, our results show a similar behavior for the samples as-cast with heat treatment and as-cast centrifuged; that is, making evident that the addition of 0.5% cobalt in the AuFe system favors the increase of the matrix-dentrite surface rate, consequently augmenting the gold-rich phase. Furthermore, we found that the longer the time for heat treatment, the larger this phase (and lesser the dentrites). The consequence of this is the augment of the formability, up to 75%, which constitutes the main message of this research.

6. Acknowledgements

We thank to CIDEMAT, GIPIMME and BIOPHYSICS research groups. We also thank the program "academic scholarship stimulus" of Vicerrectoría de Docencia of the University of Antioquia.

References

[1] C. Lee, S. Kim, D. Lee, and R. Fukamichi, "Aging effects on microstructure and GMR in Au-Co and Au-Co-X X=Cu,Ni,Fe bulk alloys," *IEEE Transactions on Magnetics*, vol. 35, no. 5, pp. 2856–2858, Sept. 1999.

[2] *Handbook of Alloy Phase Diagram*, 3rd ed., ASM International, Materials Park, Ohio, 1992.

[3] E.Bosco, P.Rizzi, and M.Baricco, "Phase transformations in au–fe melt spun alloys," *Materials Science and Engineering: A*, vol. 375–377, pp. 468–472, Jul. 2004.

[4] A.Blachowski, K.Ruebenbauer, J.Przewoźnik, and J.Żukrowskib, "Hyperfine interactions on iron nuclei in the bcc and fractally decomposed BCC/FCC mixed phase iron–gold alloys," *Journal of Alloys and Compounds*, vol. 458, no. 1-2, pp. 96–103, Jun. 2008.

[5] A. Blachowski, K. Ruebenbauer, A. Rakowska, and S. Kąc, "Fractal-like behavior of the BCC/FCC phase separation in the Iron-Gold alloys," *Journal of Microscopy*, vol. 237, no. 3, pp. 395–398, Apr. 2010.

[6] J. Fischer, "Hardening of Low-Alloyed Gold," *Journal Gold Bulletin*, vol. 38, no. 3, pp. 120–131, Sep. 2005.

[7] R. Süss, E. van der Lingen, L. Glaner, and M. du Toit, "18 carat yellow gold alloys with increased hardness," *Gold Bulletin*, vol. 37, no. 3-4, pp. 196–207, Sep. 2004.

[8] C. Cretu and E. van der Lingen, "Coloured gold alloys," *Gold Bulletin*, vol. 32, no. 4, pp. 115–126, Dec. 1999.

[9] *Standard Test Methods for Determination of Gold in Bullion by Fire Assay Cupellation Analysis*, American Society for Testing Materials, 2008.

[10] S. M. Restrepo, A. I. Echavarría, M. A.Giraldo, J. A. Calderón, and H. D. Sánchez, "Colour evolution of the oxide layer formed on the Au-25Fe AND Au-24.5Fe-0.5Co," *Revista Facultad de Ingeniería, Universidad de Antioquia*, no. 78, pp. 62–68, Mar. 2016.